



Contents lists available at ScienceDirect

# Colloids and Surfaces A: Physicochemical and Engineering Aspects

journal homepage: [www.elsevier.com/locate/colsurfa](http://www.elsevier.com/locate/colsurfa)

## Amino-modified microporous hyper-crosslinked resins for heavy metal ions adsorption

Katerina Burevska-Atkovska<sup>a</sup>, Federico Olivieri<sup>b</sup>, Roberto Avolio<sup>b</sup>, Rachele Castaldo<sup>b,\*</sup>, Mariacristina Cocca<sup>b</sup>, Maria Emanuela Errico<sup>b</sup>, Gennaro Gentile<sup>b</sup>, Anita Grozdanov<sup>a,b,\*\*</sup>

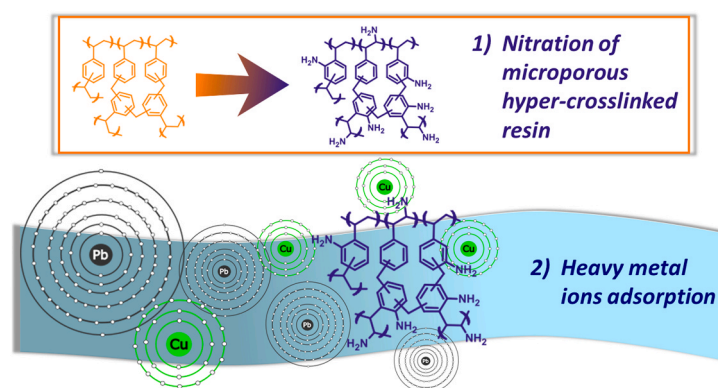
<sup>a</sup> University Ss Cyril and Methodius in Skopje – Faculty of Technology and Metallurgy, Rugjher Boskovic 16, Skopje 1000, Republic of North Macedonia

<sup>b</sup> Institute for Polymers Composites and Biomaterials, National research Council of Italy (IPCNR), Via Campi Flegrei 34, Pozzuoli, NA 80078, Italy

### HIGHLIGHTS

- Micro/mesoporous hyper-crosslinked resins were synthesized.
- Micro/mesoporous resins were functionalized with amino moieties.
- Pb and Cu ions were captured through adsorption.
- Amino-modification enhances more than 3 times the adsorption of metal ions.
- The proposed mechanism environmental relevance relies in its spontaneity, reversibility, energy- and cost-effectiveness.

### GRAPHICAL ABSTRACT



### ARTICLE INFO

#### Keywords:

Heavy metals  
Lead  
Copper  
Microporous polymers  
Amino-functionalization  
Adsorption

### ABSTRACT

In this work, a high surface area micro/mesoporous hyper-crosslinked resin based on vinylbenzyl chloride and divinylbenzene is synthesized through a solvent-free polymerization followed by Friedel-Crafts alkylation. The hyper-crosslinked resin is then functionalized with amino moieties and the effect of the functionalization on the adsorption of metal ions is evaluated. After a chemical-physical characterization of the hyper-crosslinked resins, equilibrium adsorption tests of Pb(II) and Cu(II) in water are performed. The plain and amino-modified hyper-crosslinked resins (HCLR and HCLR-NH<sub>2</sub>) exhibit specific surface area (SSA) of about 1800 m<sup>2</sup>/g and 800 m<sup>2</sup>/g, respectively. They both exhibit micro/mesoporous structure, and their pore size distribution is modified upon functionalization. The amino-functionalization, while reducing prevalently the mesoporosity of the resin, does not significantly affect the micropores. HCLR-NH<sub>2</sub> displays higher efficiency in removing both metal ions from aqueous solution compared to the unmodified resin. HCLR-NH<sub>2</sub> is able to capture up to about 70 % of Pb(II) and up to about 48 % of Cu(II) dissolved in water at 5 mg/L concentration while in the same tests, HCLR captures about 25 % of Pb(II) and 17 % of Cu(II). The resins adsorption mechanisms follow the Langmuir model,

\* Corresponding author.

\*\* Corresponding author at: University Ss Cyril and Methodius in Skopje – Faculty of Technology and Metallurgy, Rugjher Boskovic 16, Skopje 1000, Republic of North Macedonia.

E-mail addresses: [rachele.castaldo@cnr.it](mailto:rachele.castaldo@cnr.it) (R. Castaldo), [anita.grozdanov@yahoo.com](mailto:anita.grozdanov@yahoo.com) (A. Grozdanov).

<https://doi.org/10.1016/j.colsurfa.2024.134720>

Received 10 March 2024; Received in revised form 29 June 2024; Accepted 2 July 2024

Available online 3 July 2024

0927-7757/© 2024 The Authors. Published by Elsevier B.V. This is an open access article under the CC BY license (<http://creativecommons.org/licenses/by/4.0/>).

suggesting a specific and functional groups-related adsorption mechanism. Therefore, the major adsorption capacity of HCLR-NH<sub>2</sub> is to be primarily attributed to the grafted amino moieties, which establish chelating interactions with the metal cations. Overall, results assess the relevance of the micropores and the amino functionalization to capture Pb and Cu ions via adsorption.

## 1. Introduction

The development of the industry and the continuous worldwide growth of the population lead to production of the large amounts of wastewater every day. Wastewaters contain various contaminants, including heavy metals, that are amongst the most dangerous toxic pollutants. Since heavy metals are non-biodegradable, when they enter the ecosystem, through the food chain or by long term exposure, they can cause serious health problems [1].

In order to protect the environment from harmful influence of heavy metals, wastewaters must undergo appropriate treatment before discharge. Different methods have been utilized to remove heavy metals from wastewater, such as adsorption, ion exchange, membrane filtration, chemical precipitation [2–5].

Because of its simplicity, low-costs and high efficiency, adsorption is the most widely used method for heavy metals elimination from aqueous solutions. Adsorption shows great potentiality due to its ease of design and operation, low cost, high removal capacity and due to its reversibility, which allows to regenerate and reuse the adsorbent. Moreover, adsorption processes do not induce the formation of harmful substances [6].

Many conventional materials, such as clay minerals, activated carbon and zeolites have long term application as heavy metals adsorbents [7,8]. Nowadays, the goal of many researchers, in the direction of environmental protection, is to find and develop new efficient, low impact and reusable area materials for heavy metals adsorption from wastewater. Recently developed advanced adsorbents comprehend graphene-based materials [9–11], properly functionalized mesoporous silica nanoparticles [12,13], microporous polymers and hybrids such as metal organic frameworks [14], covalent organic frameworks [15], porous aromatic frameworks [16], conjugated polymers [17], polymers of intrinsic porosity [18], Schiff-based polymers, characterized by the presence of azomethine linkages in their structures [19] and hyper-crosslinked resins (HCLRs) [20–23].

In particular, hyper-crosslinked resins are very interesting as they can be properly designed and synthesized to be employed as highly efficient heavy metals adsorbents, because of their large surface area, high porosity, adjustable pore size, morphology and functionality and their thermal and chemical stability [24–26]. For example, the great advantage in using hyper-crosslinked resins for adsorption applications lies in the possibility to modulate their porous structure and functionalities by adding functional nanofillers [27,28], by inducing copolymerization with functional monomers [29] or by post-synthesis functionalization [30,31]. Indeed, specific tuning of porosity and surface chemistry are primary in order to develop functional materials with high adsorption capacity towards selected pollutants and with anti-interference ability in complex environments [32–36].

Many researches focused on the enhancement of the adsorption capacity of hyper-crosslinked resins upon the grafting of amino moieties or different N-containing functional groups on the resin structure. For instance, methylamine modified resins showed great efficiency in citric acid adsorption and desorption [37] and the adsorption of p-nitrobenzoic acid was demonstrated to be dramatically improved by modifying the polymer with amino-groups able to increase the hydrophilicity of the resin [38]. Amino-functionalized hyper-crosslinked resins have also shown high potential for CO<sub>2</sub> capture [31,39]. The effectiveness in heavy metals adsorption of these polymers is likewise reported due to amine groups capacity of anchoring metal ions [40–42]. Indeed, the interaction between metals and N-atoms is well-known [43,44] and

largely exploited for heavy metal adsorption [19,45] and other fields such as corrosion protection [46,47], which further corroborate the potentiality of the amino functionalization of the adsorbents to improve the adsorption of heavy metals.

Here, high surface area amino-functionalized hyper-crosslinked resins were prepared by a high yield and versatile procedure based on the bulk polymerization of a vinylbenzyl chloride-divinylbenzene copolymer followed by Friedel-Crafts hyper-crosslinking reaction and amino-functionalization by a nitration/reduction process. The obtained plain and amino-functionalized resins were characterized in terms of morphology and by spectroscopic and thermal analysis. Amino-functional groups were quantified through ninhydrin assay and the porous structure of the resins before and after amino-functionalization was characterized by nitrogen adsorption analysis. Finally, the effect of the amino-functionalization on the adsorption capacity of the high surface area resin towards metal ions was evaluated by equilibrium adsorption tests of Pb(II) and Cu(II). Pb and Cu were selected as target heavy metal pollutants due to their relevance in several sectors. Indeed, lead is present in several products for different applications, such as batteries [48] and radiation protective equipment [49]. Recently, solutions towards its capture and immobilization have been investigated also to solve issues related to its possible leakage from perovskite solar cells [50]. Moreover, copper is frequently present in high concentrations in wastewater as it is widely used in industrial applications, such as metal polishing, electroplating, and etching. [51].

## 2. Materials and methods

### 2.1. Reagents and chemicals

Vinylbenzyl chloride (VBC,  $\geq 95.0\%$  mixture of isomers,  $\sim 70\%$  meta +  $\sim 30\%$  para), p-divinylbenzene (DVB, 85 % meta isomer  $\sim 10\%$  wt%), 2,2'-azobis(2-methylpropionitrile) (AIBN,  $> 98\%$ ), FeCl<sub>3</sub> ( $\geq 97\%$ ), nitric acid (ACS reagent, 70 %), sulfuric acid (ACS reagent, 95.0–98.0 %), NaOH ( $\geq 97.0\%$  pellets), stannous chloride (reagent grade, 98 %), hydrochloric acid (ACS reagent, 37 %), ninhydrin, pyridine ( $\geq 99.0\%$ ), (3-aminopropyl)triethoxysilane (APTES,  $\geq 99.0\%$ ), ethanol, 1,2-dichloroethane (DCE) and all solvents were purchased by Sigma-Aldrich (Milan, Italy) and used without further purification.

The preparation of metal ions solutions was made using salts of lead nitrate (Merck) and copper (II) nitrate trihydrate (Carlo Erba Reagents). 0.1 M NaOH and 0.1 M HNO<sub>3</sub> were added to adjust the pH of the solutions. All reagents and chemicals used in the adsorption experiment were of analytical grade.

### 2.2. Synthesis and functionalization of hyper-crosslinked resins

Amino-functionalized hyper-crosslinked resins were prepared by previously reported procedure based on bulk polymerization followed by Friedel-Crafts hyper-crosslinking and a nitration/reduction process [31]. In detail, DVB and VBC were mixed in the 2/98 molar ratio under nitrogen, then 0.5 phr AIBN was added and mixing was continued for 30 min. The mixture was taken to 80 °C and polymerization was carried out for 6 h. The obtained polymer was purified with methanol and acetone, dried and then subjected to hyper-crosslinking through Friedel-Crafts reaction, promoted by FeCl<sub>3</sub>. In the specific, the precursor polymer was swollen in DCE (15 mL per gram of polymer) at room temperature for 2 hours under N<sub>2</sub> flux; then, the mixture was cooled with an ice-bath and FeCl<sub>3</sub> (0.85 phr) was added; after 2 hours, the

mixture was heated to 80 °C, promoting the hyper-crosslinking reaction. The resulting polymer (coded HCLR) was purified with water and methanol and dried in oven at 80 °C under vacuum. Then, HCLR was added to a mixture of HNO<sub>3</sub>/H<sub>2</sub>SO<sub>4</sub>/H<sub>2</sub>O (75/20/5 by volume), kept under nitrogen, in an ice bath, and stirred for 1 h. This mixture was poured slowly into a 10 M NaOH solution and then the product was purified with water until neutrality. The reduction of this product was induced by SnCl<sub>2</sub> in a HCl/ethanol equimolar solution, under nitrogen, for 2 h at 60 °C. The resulting resin was washed with a diluted H<sub>2</sub>SO<sub>4</sub> solution, neutralized with distilled water and dried. This sample was coded HCLR-NH<sub>2</sub>.

### 2.3. Morphology, chemical-physical and textural properties of the hyper-crosslinked resins

HCLR and HCLR-NH<sub>2</sub> were characterized by scanning electron microscopy using a FEI Quanta 200 FEG SEM. The hyper-crosslinked resins were deposited on aluminum stubs covered by carbon adhesive disks and the analysis was performed using a secondary electron detector and an acceleration voltage of 30 kV.

The amino-modification of the hyper-crosslinked resins was assessed by means of Fourier transform infrared (FTIR) spectroscopy and by ninhydrin assay.

FTIR analysis was performed on HCLR and HCLR-NH<sub>2</sub> in attenuated total reflectance (ATR) mode using a PerkinElmer Spectrum One FTIR spectrometer equipped with an ATR module. Measurements were performed with a resolution of 4 cm<sup>-1</sup> and 32 scan collections.

The ninhydrin assay was performed on HCLR-NH<sub>2</sub>. A ninhydrin/pyridine solution was prepared by dissolving 280 mg of ninhydrin and 10 mL of pyridine in 40 mL of ethanol; an excess of ninhydrin solution was added to a beaker containing the amino-modified resin, which was stirred, in the dark, at 90 °C for 30 min. The concentration of the Ruhemann's Blue complex formed in this condition was evaluated through UV-vis spectroscopy, using a Jasco V570 UV spectrophotometer and a previously recorded calibration curve of the Ruhemann's Blue obtained by reaction of ninhydrin with APTES in similar conditions.

Thermogravimetric analysis (TGA) was also carried out on HCLR and HCLR-NH<sub>2</sub> by using a Perkin Elmer Pyris 1 thermogravimetric analyzer. The samples were analyzed in oxidizing atmosphere, at 10 °C/min heating rate, from room temperature to 800 °C.

Gas adsorption volumetric analysis was performed on HCLR and HCLR-NH<sub>2</sub> using a Micromeritics 3Flex analyzer. Specific surface area (SSA) was determined by N<sub>2</sub> adsorption measurements at 77 K from the linear part of the Brunauer-Emmett-Teller (BET) equation. The specific pore volume was evaluated at 0.97 p/p<sup>0</sup>. Nonlocal density functional theory (NLDFT) was applied to the nitrogen adsorption isotherms to evaluate the pore size distribution of the materials. The microporous fraction was evaluated as the percent ratio of the volume of pores of width lower than 2 nm over the total pore volume of the resins. Prior to the analyses all samples were degassed at 100 °C under vacuum (P < 10<sup>-7</sup> mbar) and all the adsorption measurements were performed using high purity gases (> 99.999 %).

### 2.4. Adsorption of metal ions

Adsorption experiments were performed using batch adsorption technique. The equilibrium data were obtained for five different initial concentrations of Pb(II) and Cu(II) ions (5, 10, 15, 20 and 25 mg/L) for both examined materials. The Erlenmeyer flasks containing 100 mL of each solution with different initial Pb(II) or Cu(II) ions concentration and 0.1 g of the adsorbents were placed on the shaker (Certomat R, B. Braun by Biotech International) for continuous mixing for 5 h at 180 rpm at room temperature. Tests were performed at pH 6 for all solutions. To determine the residual concentration of Pb(II) and Cu(II) ions after the adsorption, the atomic absorption spectrophotometer (Agilent 55B AA) was utilized. Langmuir and Freundlich isotherms were applied to

process the experimental data. All experiments were conducted in triplicate; average results and standard deviation were calculated.

## 3. Results and discussion

### 3.1. Morphology, chemical-physical and textural properties of the hyper-crosslinked resins

HCLR and HCLR-NH<sub>2</sub> resins were synthesized and functionalized through bulk polymerization, hyper-crosslinking and through nitration/reduction as schematized in Fig. 1.

The resins appear as particles of irregular shape with dimension up to 40 μm, as evidenced in SEM micrographs (Fig. 2a). The amino-modification does not affect their morphology. On the other hand, the effect of the -NH<sub>2</sub> grafting on the resin chemical structure was investigated qualitatively by FTIR analysis and quantitatively by ninhydrin assay. The FTIR spectrum of HCLR-NH<sub>2</sub> (Fig. 1b) exhibits the typical absorption signals of the -NH<sub>2</sub> groups, with the broad N-H absorption band in the range 3000–3670 cm<sup>-1</sup>, the N-H bending at 1601 cm<sup>-1</sup>, the aromatic and aliphatic C-N absorption signals between 1287 and 1127 cm<sup>-1</sup> (Fig. 1a) [38]. Through the ninhydrin assay, based on the reaction of ninhydrin with primary amines, the NH<sub>2</sub> content in HCLR-NH<sub>2</sub> was found to be 2.53 ± 0.27 mmol/g. TGA analysis was performed on the plain and amino-modified resins. HCLR exhibit a slight weight gain which can be attributed to the oxidation of methylene bonds [52,53]. The amino-modified material exhibits slightly anticipated degradation in comparison to HCLR, ascribable to the thermal degradation of amino moieties (Fig. 1c) [30,31]. In this way, the amino-functionalization proposed does not affect significantly the hyper-crosslinked resin thermal properties and potential applications.

HCLR and HCLR-NH<sub>2</sub> textural properties were investigated by nitrogen adsorption analysis. HCLR exhibits the type IV IUPAC isotherm with a significant hysteresis, typical of micro/mesoporous materials (Fig. 3a) [54]. Upon functionalization, HCLR-NH<sub>2</sub> acquires a more microporous structure, characterized by the typical type I/Langmuir isotherm (Fig. 3a). Indeed, pore size distributions graphs of HCLR and HCLR-NH<sub>2</sub> show that, while the first sample presents a very wide porosity distribution, with most of the porosity included between about 1 and 10 nm, the amino-modified resin porosity prevalently ranges from 0.4 nm up to 4 nm (Fig. 3b), reaching a microporosity fraction of 72 % (Table 1). Furthermore, as also evidenced in the cumulative pore volume magnification (Fig. 3d), HCLR-NH<sub>2</sub> exhibits higher porosity in the range 0.4–1.3 nm.

Specific surface area of HCLR and HCLR-NH<sub>2</sub> were evaluated by BET and Langmuir models, and results are reported in Table 1. As anticipated, given the type of isotherms, the BET model results to be more appropriate for the plain resin and the Langmuir model is more suitable for the prevalently microporous amino-modified resin. While the total amount of porosity is reduced by the amino-functionalization (from 1.36 to 0.36 cm<sup>3</sup>/g), the above underlined increase of the content of micropores narrower than 1 nm results useful for adsorption applications both in water and air [31,55].

### 3.2. Adsorption of metal ions

The efficiency of the adsorbents on elimination of metal ions is perceived by determining the percentage of removal (R, %) using the following equation:

$$R = \frac{C_0 - C_e}{C_0} \cdot 100 \quad (1)$$

where C<sub>0</sub> (mg/L) is the initial metal ion concentration and C<sub>e</sub> (mg/L) is the equilibrium concentration.

The amount of metal ions adsorbed at equilibrium, q<sub>e</sub> (mg/g), was calculated utilizing the relation below:

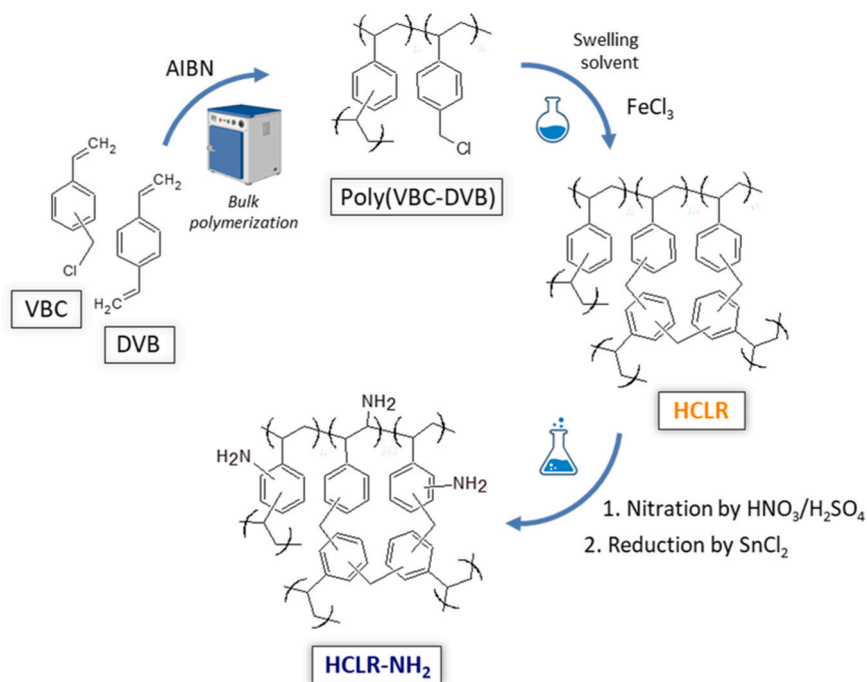


Fig. 1. Schematization of the hyper-crosslinked resins synthesis and functionalization processes.

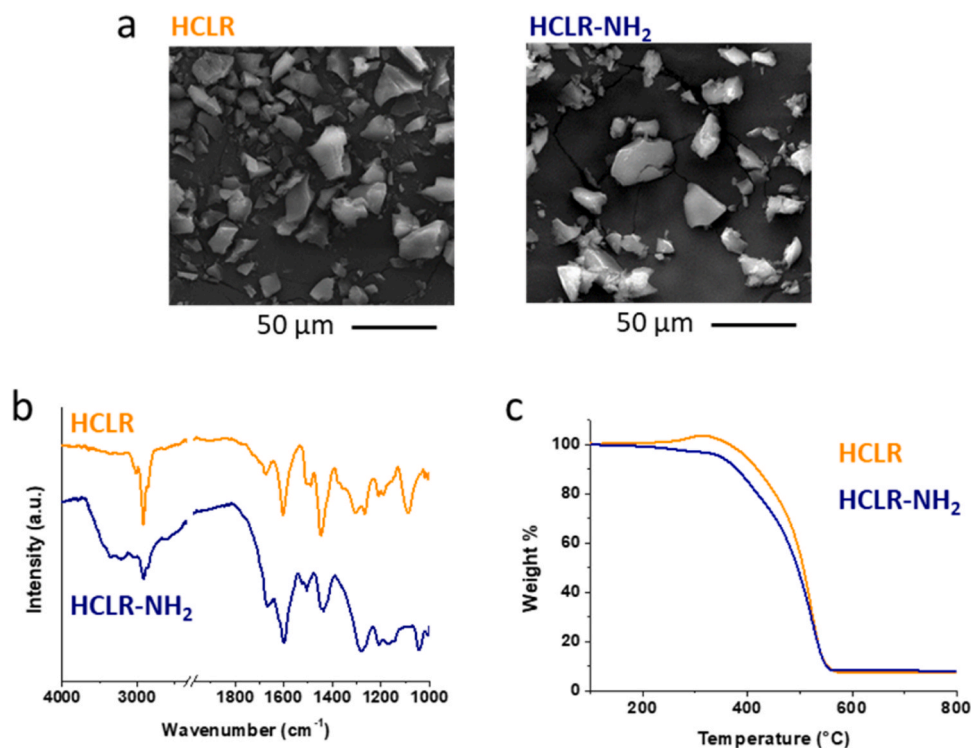


Fig. 2. SEM images (a), FTIR spectra (b) and TGA traces (c) of HCLR and HCLR-NH<sub>2</sub>.

$$q_e = \frac{(C_0 - C_e) \cdot V}{m} \quad (2)$$

where  $V$  (L) is volume of the solution and  $m$  (g) is the amount of the adsorbent.

The adsorption experiments for HCLR and HCLR-NH<sub>2</sub> were carried out with initial metal ion concentration of 5, 10, 15, 20 and 25 mg/L, using 0.1 g of adsorbents. Test were performed after assessing the

equilibrium adsorption time through repeated measure, which was found to be lower than 5 h. According to literature data, the best results for adsorption of Pb(II) and Cu(II) ions using these type of materials were achieved at pH 5–6, and therefore the adsorption tests were performed at pH 6 for all solutions [41,56,57]. The influence of the initial Pb(II) and Cu(II) ions concentration on the removal percentage for HCLR and HCLR-NH<sub>2</sub> are presented in Figs. 4a and 4b, respectively.

As shown, the amino-modified resin exhibits significantly higher



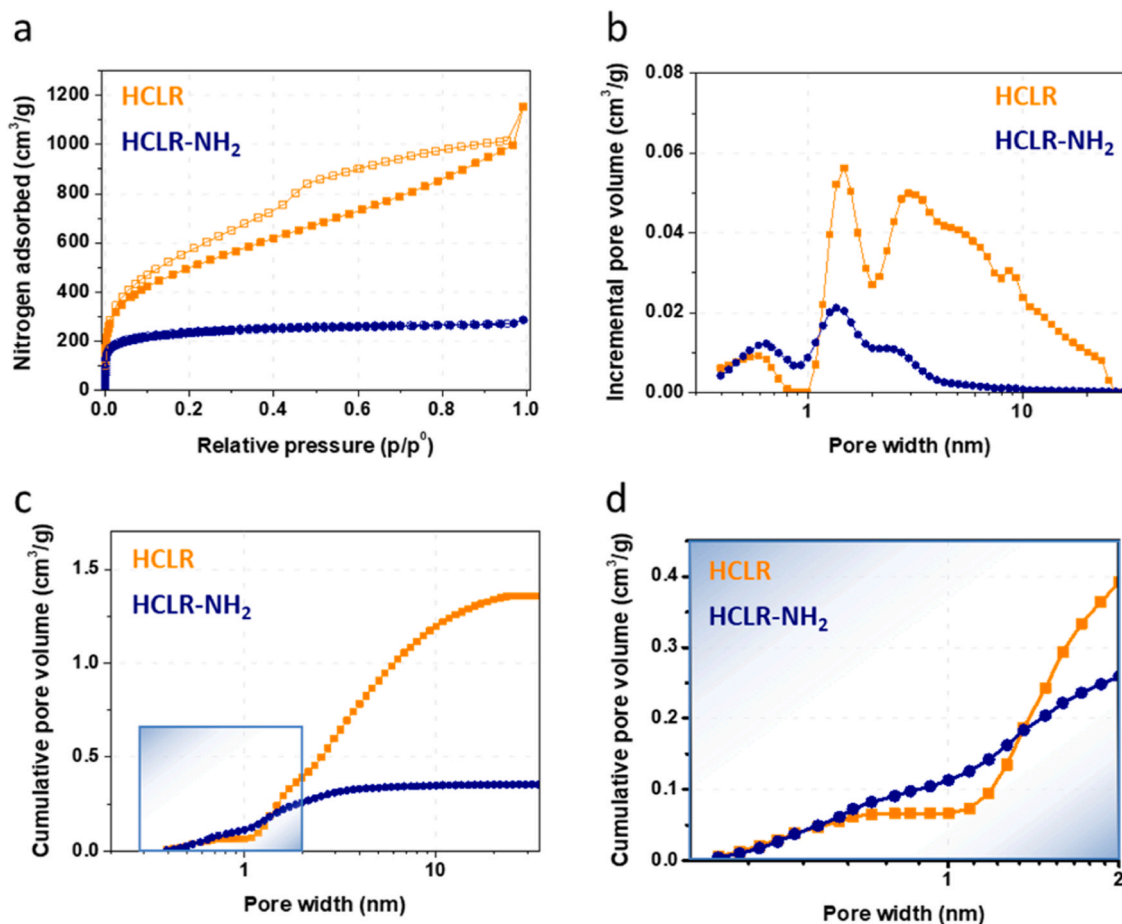


Fig. 3. Nitrogen adsorption/desorption isotherms (a), NLDFT pore size distribution (b), and cumulative pore volume (c, d) of HCLR and HCLR-NH<sub>2</sub>.

Table 1

SSA and porosity values of HCLR and HCLR-NH<sub>2</sub>.

Sample	BET specific surface area (m <sup>2</sup> /g)	Langmuir specific surface area (m <sup>2</sup> /g)	Specific pore volume (cm <sup>3</sup> /g)	Micropore fraction (%) <sup>*</sup>
HCLR	1750 ± 16	2970 ± 66	1.36	24
HCLR-NH <sub>2</sub>	819 ± 3	1140 ± 3	0.36	72

<sup>\*</sup> percentage of micropores over total pore volume

removal efficiency with respect to HCLR in all cases, capturing up to about 70 % of Pb(II) dissolved in water at 5 mg/L concentration and up to about 48 % of Cu(II) at 5 mg/L concentration. Then, the percentage of removal shows a decreasing trend as the initial concentration of metal ions increases in all cases. This trend occurs because at lower concentrations all metal ions present in the solutions are able to interact with the adsorption sites on the adsorbent surface, hence the higher efficiency of removal. At higher concentrations, because of the saturation of the adsorption sites, more metal ions remain unadsorbed in the solution. Indeed, a similar trend of the impact of initial metal ion concentration on the adsorption efficiency was reported by other researchers [40,57]. The Pb(II) removal efficiency decreases approximately from 25 % to 9 % for HCLR and from 70 % to 39 % for HCLR-NH<sub>2</sub> as the Pb(II) ions concentration increases from 5 mg/L to 25 mg/L. The same changes in the adsorption effect from the initial concentration occurs during the adsorption of copper ions. The removal efficiency of HCLR and HCLR-NH<sub>2</sub> gradually decreases approximately from 17 % to 6 % and from 48 % to 21 %, respectively, as the initial concentration of Cu(II) increases from 5 to 25 mg/L.

The initial concentration provides also a great driving force to overcome all mass transfer resistance of metal ions between the aqueous and solid phases [58]. Hence, with increasing the initial concentration of metal ions in solution, the adsorption capacity  $q_e$  of the resins increases (Fig. 4c-d). As seen in Fig. 4c, when the initial Pb(II) ions concentration increases from 5 to 25 mg/L, the adsorption capacity of HCLR increases from  $1.34 \pm 0.15$  mg/g to  $2.30 \pm 0.25$  mg/g and for the amino-functionalized resin, HCLR-NH<sub>2</sub>, the uptake increase is more significant, from  $3.77 \pm 0.21$  mg/g to  $9.88 \pm 0.23$  mg/g.

Fig. 4d shows the same increasing trend of the adsorption capacity for Cu(II) ions influenced by the increasing of the initial metal ion concentration from 5 to 25 mg/L, and it changes gradually from  $0.85 \pm 0.06$  mg/g to  $1.63 \pm 0.11$  mg/g for HCLR and from  $2.42 \pm 0.09$ – $5.44 \pm 0.13$  mg/g for HCLR-NH<sub>2</sub>.

The results of the adsorption tests show the comparison of the efficiency between HCLR and the amino-modified resin, HCLR-NH<sub>2</sub>, for Pb(II) and Cu(II) adsorption. The amino-modified material is more effective, exhibiting higher values of removal percentage as well as of adsorption capacities at all concentrations for both metal ions. This was due to the possible ions chelation with amino groups and to the presence, upon modification, of a higher microporous fraction in the HCLR-NH<sub>2</sub> resin than in HCLR [31,59,60].

Adsorption isotherms are important for adsorption equilibrium description. The Langmuir and Freundlich isotherm models, which are the most frequently used models for practical application, are employed in this study to describe the adsorption behavior. The Langmuir adsorption isotherm applies to monolayer sorption without interaction between adsorbed molecules. Its linear form is represented by the following equation:

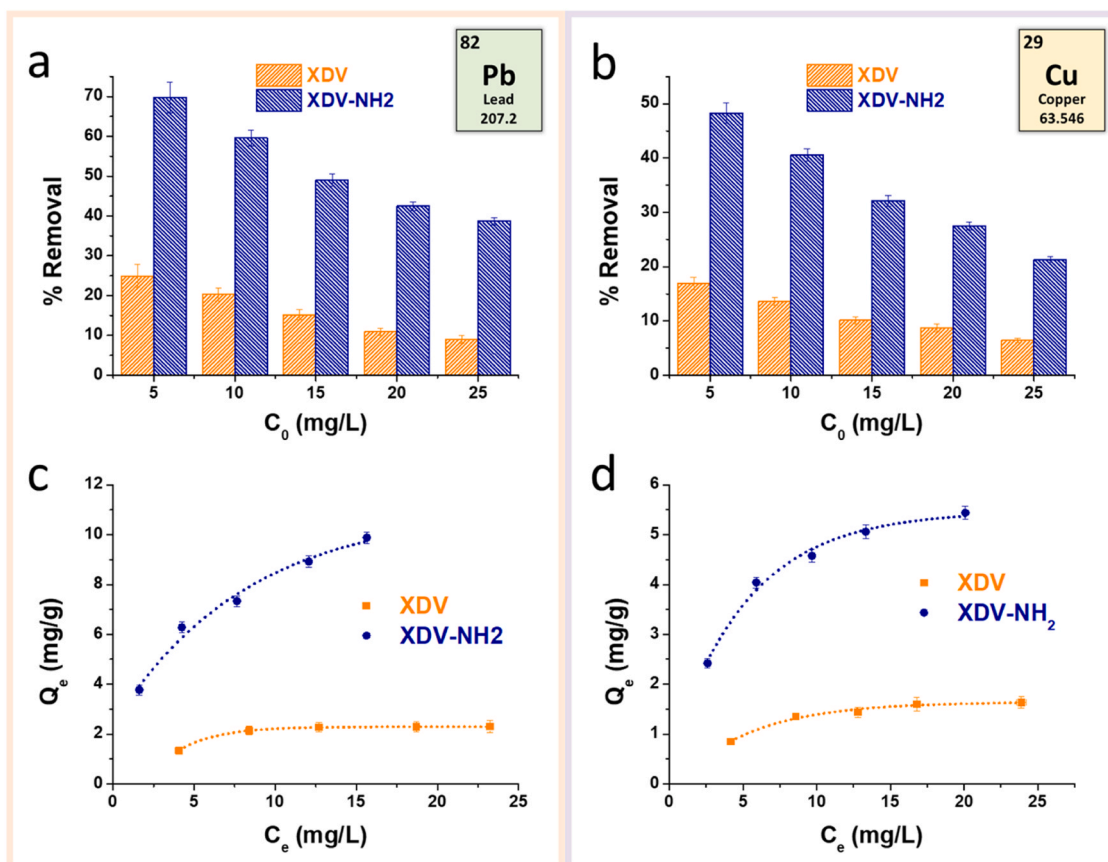


Fig. 4. Effect of initial concentration on adsorption of Pb(II) (a) and Cu(II) (b) on HCLR and HCLR-NH<sub>2</sub>, Pb(II) (c) and Cu(II) (d) equilibrium adsorption isotherms of HCLR and HCLR-NH<sub>2</sub>.

$$\frac{C_e}{q_e} = \frac{1}{q_m \cdot b} + \frac{C_e}{q_m} \quad (3)$$

where  $q_m$  [mg/g] is the maximum adsorption capacity while  $b$  [l/mg] is the Langmuir equilibrium constant.

The dependence of  $C_e/q_e$  vs.  $C_e$  for Pb(II) and Cu(II) adsorption onto HCLR and HCLR-NH<sub>2</sub> are shown in Fig. 5a-b.

The first empirical equation of an adsorption isotherm is given by Freundlich and it is applicable for monolayer and multilayer adsorption. Its linear form has the following expression:

$$\log q_e = 1/n \cdot \log C_e + \log K_F \quad (4)$$

where  $K_F$  [mg/g] is the Freundlich constant and  $n$  is empirical parameter related to the intensity of adsorption.

The linear Freundlich plots for Pb(II) and Cu(II) adsorption onto HCLR and HCLR-NH<sub>2</sub> are given in Fig. 5c-d.

Using the equations on the graphs above, maximum adsorption capacities,  $q_m$ , the Langmuir equilibrium constant,  $b$ , the Freundlich constant,  $K_F$ , and the empirical parameter,  $n$ , were calculated and their values as well as the values of the correlation coefficients,  $R^2$ , are presented in Table 2.

The obtained values of the maximum adsorption capacity,  $q_m$ , from Langmuir isotherm, and the Freundlich constant,  $K_F$ , show that HCLR-NH<sub>2</sub>, has higher adsorption capacity than HCLR, which confirms the previous conclusion on greater efficiency of the modified material for removal of the Pb(II) and Cu(II) ions than its unmodified form at the same experimental conditions. These results also indicate a greater sorption capacity for Pb(II) than for Cu(II), in accordance with literature data [41], which is due to the higher atomic weight of Pb with respect to Cu. Indeed, if considered the molar amounts, Cu(II) is adsorbed in higher extent than Pb(II), probably due to the higher coordination number, i.e.

the number of amine groups that coordinate each metal ion, showed by Pb(II) in comparison to Cu(II) [61].

The linearity of the plots as well as the higher values of the coefficients of correlation, ( $R^2 > 0.98$ ) indicate that the Langmuir isotherm fits better than the Freundlich isotherm, for both examined materials and for both metal ions. These trends clearly indicate that the adsorption of Pb(II) and Cu(II) takes place prevalently in small micropores in HCLR and HCLR-NH<sub>2</sub> and through specific site interactions. Therefore, large mesopores present in HCLR do not contribute significantly to the adsorption of metal ions. In particular, in the amino-modified resin, it is likely that adsorption of metal ions takes place due to chelation with the amino functionalities, explaining the greater uptake of HCLR-NH<sub>2</sub> with respect to HCLR. Therefore, the amino-functionalization here proposed is particularly suitable for the application of hyper-crosslinked resins as metal ions adsorbents. Indeed, although with the amino-functionality process it is associated a reduction in total pore volume of the high surface area resin, this factor does not affect the hyper-crosslinked resin capacity to adsorb metal ions. On the other hand, the grafting of -NH<sub>2</sub> groups on the hyper-crosslinked resin structure allows to greatly enhance the adsorption of metal ions such as Pb(II) and Cu(II), more than 4 and 3 times, respectively, with respect to the unmodified high SSA hyper-crosslinked resin.

The maximum uptake of the metal ions here tested by the amino-functionalized hyper-crosslinked resin HCLR-N<sub>2</sub>,  $5.44 \pm 0.13$  mg/g for Cu(II) and  $9.88 \pm 0.23$  mg/L for Pb(II), fit in the middle of the range of performances of literature materials [40]. It is to note that the adsorption capacity of these resins depends on experimental conditions such as dosing ratio (mass of adsorbent per volume of metal salt solution) and the initial concentration of the metal salt solution. Also, the equilibrium adsorption curves of HCLR-NH<sub>2</sub> have not reached plateau values yet, especially in the case of Pb adsorption (Fig. 4c,d), therefore an increase

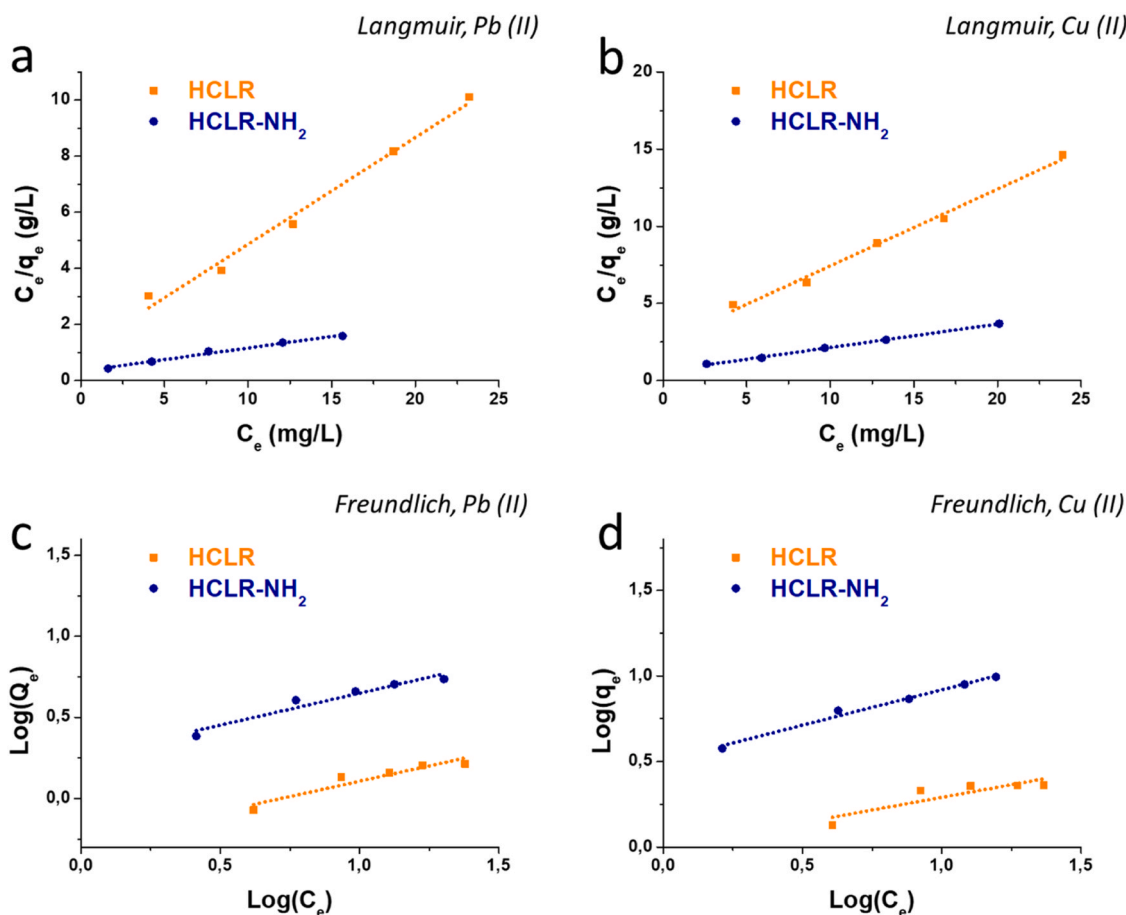


Fig. 5. Langmuir (a,b) and Freundlich (c,d) adsorption models for Pb(II) (a,c) and Cu(II) (b,d) adsorption on HCLR and HCLR-NH<sub>2</sub>.

Table 2

Parameters of the Langmuir and Freundlich isotherms.

Metal ion	Adsorbent	Langmuir isotherm			Freundlich isotherm		
		$q_m$ [mg/g]	$b$	$R^2$	$K_F$ [mg/g]	$n$	$R^2$
Pb(II)	HCLR	2.63	0.361	0.989	0.989	3.38	0.784
	HCLR-NH <sub>2</sub>	12.1	0.245	0.989	3.19	2.41	0.987
Cu(II)	HCLR	2.01	0.202	0.992	0.535	2.67	0.903
	HCLR-NH <sub>2</sub>	6.59	0.241	0.998	1.80	2.54	0.939

of  $Q_e$  with increasing the initial metal salt concentration ( $C_0$ ) is expected. On the other hand, HCLR-N<sub>2</sub> performance in these conditions is lower than commercial cation exchange resins developed for heavy metals adsorption [62]. In summary, the developed hyper-crosslinked resins show very high specific surface area and high amount of microporosity, which is a very good premise for adsorption application; further improvement of the functionalization extent is needed in order to reach competitive heavy metal adsorption performances with state-of-art materials.

#### 4. Conclusion

In this study, vinylbenzyl chloride/divinylbenzene-based hyper-crosslinked resins were synthesized through bulk polymerization and Friedel-Crafts alkylation and then functionalized with amino moieties. The obtained materials are micro/mesoporous resins characterized by high SSA and different functionalities. Although the amino-modification

induces a decrease of the resin SSA and total pore volume, it does not affect significantly the micropores.

The hyper-crosslinked resins chemical and textural properties were correlated to their adsorption capacities of heavy metal ions. HCLR and HCLR-NH<sub>2</sub> were tested for the adsorption of Pb(II) and Cu(II). The Langmuir and Freundlich isotherm models were employed to study the equilibrium data and the results show that the Langmuir model provides better correspondence for all systems adsorbent/metal ion.

The amino functionalized microporous resin HCLR-NH<sub>2</sub> exhibited higher efficiency than the unmodified HCLR, more than 4 and 3 times, respectively, in removing Pb(II) and Cu(II) from aqueous solutions. This is to be primary attributed to the grafted amino moieties, which establish chelating interactions with the metal cations. Therefore, the decrease of total pore volume registered upon the amino functionalization is not detrimental for the adsorption of metal ions and the proposed approach is suitable for the realization of high surface area hyper-crosslinked resins for the adsorption of heavy metal ions.

#### CRediT authorship contribution statement

**Katerina Burevska-Atkovska:** Writing – review & editing, Writing – original draft, Methodology, Investigation, Conceptualization. **Roberto Avolio:** Writing – review & editing, Methodology, Investigation. **Federico Olivieri:** Writing – review & editing, Writing – original draft, Validation, Methodology, Investigation, Conceptualization. **Anita Grozdanov:** Writing – review & editing, Writing – original draft, Visualization, Validation, Supervision, Methodology, Conceptualization. **Mariacristina Cocca:** Writing – review & editing, Validation, Supervision, Methodology. **Rachele Castaldo:** Writing – review & editing, Writing – original draft, Visualization, Validation, Supervision,

Methodology, Conceptualization. **Gennaro Gentile**: Writing – review & editing, Visualization, Supervision, Methodology, Conceptualization. **Maria Emanuela Errico**: Writing – review & editing, Validation, Methodology.

### Declaration of Competing Interest

The authors declare that they have no known competing financial interests or personal relationships that could have appeared to influence the work reported in this paper.

### Data Availability

Data will be made available on request.

### References

- [1] K. Rehman, F. Fatima, I. Waheed, M.S.H. Akash, Prevalence of exposure of heavy metals and their impact on health consequences, *J. Cell. Biochem.* 119 (2018) 157–184.
- [2] R.J. Stephenson, S.J.B. Duff, Coagulation and precipitation of a mechanical pulping effluent—I. Removal of carbon, colour and turbidity, *Water Res* 30 (1996) 781–792.
- [3] H. Xiang, X. Min, C.-J. Tang, M. Sillanpää, F. Zhao, Recent advances in membrane filtration for heavy metal removal from wastewater: a mini review, *J. Water Process Eng.* 49 (2022) 103023.
- [4] J. Du, B. Zhang, J. Li, B. Lai, Decontamination of heavy metal complexes by advanced oxidation processes: a review, *Chin. Chem. Lett.* 31 (2020) 2575–2582.
- [5] A. Dąbrowski, Z. Hubicki, P. Podkościelny, E. Robens, Selective removal of the heavy metal ions from waters and industrial wastewaters by ion-exchange method, *Chemosphere* 56 (2004) 91–106.
- [6] X. Yang, Y. Wan, Y. Zheng, F. He, Z. Yu, J. Huang, H. Wang, Y.S. Ok, Y. Jiang, B. Gao, Surface functional groups of carbon-based adsorbents and their roles in the removal of heavy metals from aqueous solutions: a critical review, *Chem. Eng. J.* 366 (2019) 608–621.
- [7] D. Ewis, M.M. Ba-Abbad, A. Benamor, M.H. El-Naas, Adsorption of organic water pollutants by clays and clay minerals composites: a comprehensive review, *Appl. Clay Sci.* 229 (2022) 106686.
- [8] E.A. Deliyanni, G.Z. Kyzas, K.S. Triantafyllidis, K.A. Matis, Activated carbons for the removal of heavy metal ions: a systematic review of recent literature focused on lead and arsenic ions, *Open Chem.* 13 (2015) 699–708.
- [9] H. Wang, X. Yuan, Y. Wu, H. Huang, G. Zeng, Y. Liu, X. Wang, N. Lin, Y. Qi, Adsorption characteristics and behaviors of graphene oxide for Zn (II) removal from aqueous solution, *Appl. Surf. Sci.* 279 (2013) 432–440.
- [10] R. Castaldo, R. Avolio, M. Cocca, M.E. Errico, M. Lavorgna, J. Šalplachta, C. Santillo, G. Gentile, Hierarchically porous hydrogels and aerogels based on reduced graphene oxide, montmorillonite and hyper-crosslinked resins for water and air remediation, *Chem. Eng. J.* 430 (2022), <https://doi.org/10.1016/j.cej.2021.133162>.
- [11] R. Castaldo, G.C. Lama, P. Aprea, G. Gentile, M. Lavorgna, V. Ambrogio, P. Cerruti, Effect of the oxidation degree on self-assembly, adsorption and barrier properties of nano-graphene, *Microporous Mesoporous Mater.* 260 (2018) 102–115, <https://doi.org/10.1016/j.micromeso.2017.10.026>.
- [12] M.A. Khan, M. Shaheer Akhtar, O.B. Yang, Synthesis, characterization and application of sol-gel derived mesoporous TiO<sub>2</sub> nanoparticles for dye-sensitized solar cells, *Sol. Energy* 84 (2010) 2195–2201, <https://doi.org/10.1016/j.solener.2010.08.008>.
- [13] M. Guerritore, F. Olivieri, R. Avolio, R. Castaldo, M. Cocca, M.E. Errico, M. Lavorgna, B. Silvestri, V. Ambrogio, G. Gentile, Hierarchical micro-to-macroporous silica nanoparticles obtained by their grafting with hyper-crosslinked resin, *Microporous Mesoporous Mater.* 335 (2022) 111864, <https://doi.org/10.1016/j.micromeso.2022.111864>.
- [14] G.-R. Xu, Z.-H. An, K. Xu, Q. Liu, R. Das, H.-L. Zhao, Metal organic framework (MOF)-based micro/nanoscaled materials for heavy metal ions removal: The cutting-edge study on designs, synthesis, and applications, *Coord. Chem. Rev.* 427 (2021) 213554.
- [15] N.W. Ockwig, A.P. Co, M.O. Keeffe, A.J. Matzger, O.M. Yaghi, Porous, Crystalline, Covalent Org. Framework. 310 (2005) 1166–1171.
- [16] Y. Tian, G. Zhu, Porous aromatic frameworks (PAFs), *Chem. Rev.* 120 (2020) 8934–8986.
- [17] X. Wang, Y. Zhao, L. Wei, C. Zhang, J.-X. Jiang, Nitrogen-rich conjugated microporous polymers: impact of building blocks on porosity and gas adsorption, *J. Mater. Chem. A.* 3 (2015) 21185–21193.
- [18] N.B. Mc Keown, P.M. Budd, Polymers of intrinsic microporosity (PIMs): Organic materials for membrane separations, heterogeneous catalysis and hydrogen storage, *Chem. Soc. Rev.* 35 (2006) 675–683, <https://doi.org/10.1039/b600349d>.
- [19] R. Sandín, M. González-Lucas, P.A. Sobarzo, C.A. Terraza, E.M. Maya, Microwave-assisted melamine-based polyaminals and their application for metal cations adsorption, *Eur. Polym. J.* 155 (2021), <https://doi.org/10.1016/j.eurpolymj.2021.110562>.
- [20] L. Tan, B. Tan, Hypercrosslinked porous polymer materials: design, synthesis, and applications, *Chem. Soc. Rev.* 46 (2017) 3322–3356, <https://doi.org/10.1039/c6cs00851h>.
- [21] R. Castaldo, G. Gentile, M. Avella, C. Carfagna, V. Ambrogio, Microporous hyper-crosslinked polystyrenes and nanocomposites with high adsorption properties: A review, *Polym. (Basel)* 9 (2017), <https://doi.org/10.3390/polym9120651>.
- [22] R. Castaldo, I. Berezovska, M.S. Silverstein, G. Gentile, PolyHIPES Containing Hyper-Cross-Linked Resins: Hierarchical Porosity with Broad and Versatile Sorption Properties, *ACS Appl. Polym. Mater.* (2023), <https://doi.org/10.1021/acscpm.3c00974>.
- [23] M. Salzano de Luna, R. Castaldo, R. Altobelli, L. Gioiella, G. Filippone, G. Gentile, V. Ambrogio, Chitosan hydrogels embedding hyper-crosslinked polymer particles as reusable broad-spectrum adsorbents for dye removal, *Carbohydr. Polym.* 177 (2017) 347–354, <https://doi.org/10.1016/j.carbpol.2017.09.006>.
- [24] R. Castaldo, R. Avolio, M. Cocca, G. Gentile, M.E. Errico, M. Avella, C. Carfagna, V. Ambrogio, A versatile synthetic approach toward hyper-cross-linked styrene-based polymers and nanocomposites, *Macromolecules* 50 (2017) 4132–4143, <https://doi.org/10.1021/acs.macromol.7b00812>.
- [25] R. Castaldo, R. Avolio, M. Cocca, G. Gentile, M.E. Errico, M. Avella, C. Carfagna, V. Ambrogio, Synthesis and adsorption study of hyper-crosslinked styrene-based nanocomposites containing multi-walled carbon nanotubes, *RSC Adv.* 7 (2017) 6865–6874, <https://doi.org/10.1039/c6ra25481k>.
- [26] J.-H. Ahn, J.-E. Jang, C.-G. Oh, S.-K. Ihm, J. Cortez, D.C. Sherrington, Rapid generation and control of microporosity, bimodal pore size distribution, and surface area in Davankov-type hyper-cross-linked resins, *Macromolecules* 39 (2006) 627–632.
- [27] M. Guerritore, R. Castaldo, B. Silvestri, R. Avolio, M. Cocca, M.E. Errico, M. Avella, G. Gentile, V. Ambrogio, Hyper-crosslinked polymer nanocomposites containing mesoporous silica nanoparticles with enhanced adsorption towards polar dyes, *Polymers* 12 (2020) 1–11, <https://doi.org/10.3390/polym12061388>.
- [28] R. Castaldo, M. Iuliano, M. Cocca, V. Ambrogio, G. Gentile, M. Sarno, A new route for low pressure and temperature CWAO: A PtRu/MoS<sub>2</sub> hyper-crosslinked nanocomposite, *Nanomaterials* 9 (2019) 1–18, <https://doi.org/10.3390/nano9101477>.
- [29] D. Bratkowska, R.M. Marcé, P.A.G. Cormack, D.C. Sherrington, F. Borrull, N. Fontanal, Synthesis and application of hypercrosslinked polymers with weak cation-exchange character for the selective extraction of basic pharmaceuticals from complex environmental water samples, *J. Chromatogr. A.* 1217 (2010) 1575–1582, <https://doi.org/10.1016/j.chroma.2010.01.037>.
- [30] R. Castaldo, V. Ambrogio, R. Avolio, M. Cocca, G. Gentile, M. Emanuela Errico, M. Avella, Functional hyper-crosslinked resins with tailored adsorption properties for environmental applications, *Chem. Eng. J.* 362 (2019) 497–503, <https://doi.org/10.1016/j.cej.2019.01.054>.
- [31] R. Castaldo, R. Avolio, M. Cocca, M.E. Errico, M. Avella, G. Gentile, Amino-functionalized hyper-crosslinked resins for enhanced adsorption of carbon dioxide and polar dyes, *Chem. Eng. J.* 418 (2021), <https://doi.org/10.1016/j.cej.2021.129463>.
- [32] Y. Zhang, Y. Feng, Q. Xiang, F. Liu, C. Ling, F. Wang, Y. Li, A. Li, A high-flux and anti-interference dual-functional membrane for effective removal of Pb(II) from natural water, *J. Hazard. Mater.* 384 (2020) 121492, <https://doi.org/10.1016/j.jhazmat.2019.121492>.
- [33] C. Ling, Z. Ren, M. Wei, F. Tong, Y. Cheng, X. Zhang, F. Liu, Highly selective removal of Ni(II) from plating rinsing wastewaters containing [Ni-xNH<sub>3</sub>-yP2O7]n complexes using N-chelating resins, *J. Hazard. Mater.* 398 (2020) 122960, <https://doi.org/10.1016/j.jhazmat.2020.122960>.
- [34] Y. Feng, G. Chen, Y. Zhang, D. Li, C. Ling, Q. Wang, G. Liu, Superhigh co-adsorption of tetracycline and copper by the ultrathin g-C<sub>3</sub>N<sub>4</sub> modified graphene oxide hydrogels, *J. Hazard. Mater.* 424 (2022) 127362, <https://doi.org/10.1016/j.jhazmat.2021.127362>.
- [35] Q. Liu, P. Feng, L. Shao, X. Liu, C. Chen, J. Lu, C. Ling, Y. Zhang, D. Sun, Q. Ran, Ultra-purification of heavy metals and robustness of calcium silicate hydrate (C–S–H) nanocomposites, *Chemosphere* 335 (2023) 139063, <https://doi.org/10.1016/j.chemosphere.2023.139063>.
- [36] Y. Lv, L. Zong, Z. Liu, J. Du, F. Wang, Y. Zhang, C. Ling, F. Liu, Sequential separation of Cu(II)/Ni(II)/Fe(II) from strong-acidic pickling wastewater with a two-stage process based on a bi-pyridine chelating resin, *Chin. Chem. Lett.* 32 (2021) 2792–2796, <https://doi.org/10.1016/j.ccl.2021.01.038>.
- [37] X. Peng, P. Yang, K. Dai, Y. Chen, X. Chen, W. Zhuang, H. Ying, J. Wu, Synthesis, adsorption and molecular simulation study of methylamine-modified hyper-cross-linked resins for efficient removal of citric acid from aqueous solution, *Sci. Rep.* 10 (2020) 9623, <https://doi.org/10.1038/s41598-020-66592-8>.
- [38] C. Xu, C. Wang, W. Sun, W. Yu, C. Yin, F. Liu, M. Xian, S. Yu, Preparation of hypercrosslinked amine modification resin and its adsorption properties for nitroaromatics, *Environ. Sci. Pollut. Res.* 26 (2019) 10767–10775, <https://doi.org/10.1007/s11356-019-04370-4>.
- [39] F. Liu, S. Wang, G. Lin, S. Chen, Development and characterization of amine-functionalized hyper-cross-linked resin for CO<sub>2</sub> capture, *N. J. Chem.* 42 (2018) 420–428, <https://doi.org/10.1039/c7nj03421k>.
- [40] H. Masoumi, A. Ghaemi, H.G. Gilani, Evaluation of hyper-cross-linked polymers performances in the removal of hazardous heavy metal ions: A review, *Sep. Purif. Technol.* 260 (2021) 118221.
- [41] Z. Yang, X. Huang, X. Yao, H. Ji, Thiourea modified hyper-crosslinked polystyrene resin for heavy metal ions removal from aqueous solutions, *J. Appl. Polym. Sci.* 135 (2018) 1–13, <https://doi.org/10.1002/app.45568>.
- [42] Y. He, Q. Liu, J. Hu, C. Zhao, C. Peng, Q. Yang, H. Wang, H. Liu, Efficient removal of Pb(II) by amine functionalized porous organic polymer through post-synthetic



- modification, *Sep. Purif. Technol.* 180 (2017) 142–148, <https://doi.org/10.1016/j.seppur.2017.01.026>.
- [43] W. Xia, Interactions between metal species and nitrogen-functionalized carbon nanotubes, *Catal. Sci. Technol.* 6 (2016) 630–644.
- [44] M.A. Gleeson, A.W. Kleyn, Nitrogen interactions at metal surfaces, *Nucl. Instrum. Methods Phys. Res. Sect. B Beam Interact. Mater. At.* 317 (2013) 109–114.
- [45] X. He, J. Xia, J. He, K. Qi, A. Peng, Y. Liu, Highly efficient capture of heavy metal ions on amine-functionalized porous polymer gels, *Gels* 9 (2023), <https://doi.org/10.3390/gels9040297>.
- [46] F. Olivieri, R. Castaldo, M. Cocca, G. Gentile, M. Lavorgna, Mesoporous silica nanoparticles as carriers of active agents for smart anticorrosive organic coatings: a critical review, *Nanoscale* 13 (2021) 9091–9111, <https://doi.org/10.1039/d1nr01899j>.
- [47] F. Olivieri, R. Castaldo, M. Cocca, G. Gentile, M. Lavorgna, Innovative silver-based capping system for mesoporous silica nanocarriers able to exploit a twofold anticorrosive mechanism in composite polymer coatings: tailoring benzotriazole release and capturing chloride ions, *ACS Appl. Mater. Interfaces* 13 (2021) 48141–48152, <https://doi.org/10.1021/acsami.1c15231>.
- [48] K. Raj, A.P. Das, Lead pollution: Impact on environment and human health and approach for a sustainable solution (Environmental Chemistry and Ecotoxicology), *Environ. Chem. Ecotoxicol.* 5 (2023) 79–85, <https://doi.org/10.1016/j.encco.2023.02.001>.
- [49] F. Olivieri, R. Avolio, A. Mazzone, R. Rizzi, M. Nacucchi, R. Castaldo, L. Ambrosio, High filler content acrylonitrile-butadiene-styrene composites containing tungsten and bismuth oxides for effective lead-free x-ray radiation shielding, (2023) 1–13. (<https://doi.org/10.1002/pc.27906>).
- [50] H. Zhang, J. Lee, G. Nasti, R. Handy, A. Abate, M. Grätzel, N. Park, Lead immobilization for environmentally sustainable perovskite solar cells 617 (2023) 687–695, <https://doi.org/10.1038/s41586-023-05938-4>.
- [51] N. Hafizah, A. Hamid, M. Iqbal, M. Tahir, A. Chowdhury, A.H. Nordin, A. A. Alshaikh, M.A. Suid, N.I. Nazaruddin, N.D. Nozaizeli, S. Sharma, A.I. Rushdan, The Current State-Of-Art of Copper Removal from Wastewater: A Review, *Water* 14 (2022) 3086, <https://doi.org/10.3390/w14193086>.
- [52] J. Guadalupe, A.M. Ray, E.M. Maya, B. Gómez-Lor, M. Iglesias, Truxene-based porous polymers: From synthesis to catalytic activity, *Polym. Chem.* 9 (2018) 4585–4595, <https://doi.org/10.1039/c8py01082j>.
- [53] E.S. Sanz-Pérez, L. Rodríguez-Jardón, A. Arencibia, R. Sanz, M. Iglesias, E.M. Maya, Bromine pre-functionalized porous polyphenylenes: new platforms for one-step grafting and applications in reversible CO<sub>2</sub> capture, *J. CO<sub>2</sub> Util.* 30 (2019) 183–192, <https://doi.org/10.1016/j.jcou.2019.02.005>.
- [54] M. Thommes, K. Kaneko, A.V. Neimark, J.P. Olivier, F. Rodriguez-Reinoso, J. Rouquerol, K.S.W. Sing, Physisorption of gases, with special reference to the evaluation of surface area and pore size distribution (IUPAC Technical Report), *Pure Appl. Chem.* 87 (2015) 1051–1069, <https://doi.org/10.1515/pac-2014-1117>.
- [55] M. Sevilla, J.B. Parra, A.B. Fertes, Assessment of the role of micropore size and N-doping in CO<sub>2</sub> capture by porous carbons, *ACS Appl. Mater. Interfaces* 5 (2013) 6360–6368.
- [56] B. Li, F. Su, H.K. Luo, L. Liang, B. Tan, Hypercrosslinked microporous polymer networks for effective removal of toxic metal ions from water, *Microporous Mesoporous Mater.* 138 (2011) 207–214, <https://doi.org/10.1016/j.micromeso.2010.08.023>.
- [57] A.M. Metwally, H.A. ElKhawaga, A.F.F. Shaaban, L.M. Reda, Suspension polymerization for synthesis of new hypercrosslinked polymers nanoparticles for removal of copper ions from aqueous solutions, *Polym. Bull.* (2022), <https://doi.org/10.1007/s00289-022-04654-9>.
- [58] N. Ertugay, Y.K. Bayhan, Biosorption of Cr(VI) from aqueous solutions by biomass of *Agaricus bisporus*, *J. Hazard. Mater.* 154 (2008) 432–439.
- [59] L. Zhang, C. Yu, W. Zhao, Z. Hua, H. Chen, L. Li, J. Shi, Preparation of multi-amine-grafted mesoporous silicas and their application to heavy metal ions adsorption, *J. Non Cryst. Solids* 353 (2007) 4055–4061.
- [60] W. Gong, K. Zheng, C. Zhang, L. Liu, Y. Shan, J. Yao, Simultaneous and efficient removal of heavy metal ions and organophosphorus by amino-functionalized cellulose from complex aqueous media, *J. Clean. Prod.* 367 (2022) 133040.
- [61] L.V.A. Gurgel, L.F. Gil, Adsorption of Cu(II), Cd(II), and Pb(II) from aqueous single metal solutions by succinylated mercerized cellulose modified with triethylenetetramine, *Carbohydr. Polym.* 77 (2009) 142–149, <https://doi.org/10.1016/j.carbpol.2008.12.014>.
- [62] O. Hamdaoui, Removal of copper(II) from aqueous phase by Purolite C100-MB cation exchange resin in fixed bed columns: modeling, *J. Hazard. Mater.* 161 (2009) 737–746, <https://doi.org/10.1016/j.jhazmat.2008.04.016>.